Toxicology and Applied Pharmacology 259 (2012) 74–86

Contents lists available at SciVerse ScienceDirect

Toxicology and Applied Pharmacology

journal homepage: www.elsevier.com/locate/ytaap

Pulmonary toxicity after exposure to military-relevant heavy metal tungsten alloy particles ☆

Erik Q. Roedel [a], Danielle E. Cafasso [a], Karen W.M. Lee [b], Lisa M. Pierce [b,*]

[a] Department of General Surgery, Tripler Army Medical Center, Honolulu, HI 96859, USA
[b] Department of Clinical Investigation, Tripler Army Medical Center, Honolulu, HI 96859, USA

ARTICLE INFO

Article history:
Received 21 October 2011
Revised 6 December 2011
Accepted 8 December 2011
Available online 16 December 2011

Keywords:
Tungsten alloy
Pulmonary toxicity
Inflammation
Lung macrophage
Gene expression
Oxidative burst

ABSTRACT

Significant controversy over the environmental and public health impact of depleted uranium use in the Gulf War and the war in the Balkans has prompted the investigation and use of other materials including heavy metal tungsten alloys (HMTAs) as nontoxic alternatives. Interest in the health effects of HMTAs has peaked since the recent discovery that rats intramuscularly implanted with pellets containing 91.1% tungsten/6% nickel/2.9% cobalt rapidly developed aggressive metastatic tumors at the implantation site. Very little is known, however, regarding the cellular and molecular mechanisms associated with the effects of inhalation exposure to HMTAs despite the recognized risk of this route of exposure to military personnel. In the current study military-relevant metal powder mixtures consisting of 92% tungsten/5% nickel/3% cobalt (WNiCo) and 92% tungsten/5% nickel/3% iron (WNiFe), pure metals, or vehicle (saline) were instilled intratracheally in rats. Pulmonary toxicity was assessed by cytologic analysis, lactate dehydrogenase activity, albumin content, and inflammatory cytokine levels in bronchoalveolar lavage fluid 24 h after instillation. The expression of 84 stress and toxicity-related genes was profiled in lung tissue and bronchoalveolar lavage cells using real-time quantitative PCR arrays, and *in vitro* assays were performed to measure the oxidative burst response and phagocytosis by lung macrophages. Results from this study determined that exposure to WNiCo and WNiFe induces pulmonary inflammation and altered expression of genes associated with oxidative and metabolic stress and toxicity. Inhalation exposure to both HMTAs likely causes lung injury by inducing macrophage activation, neutrophilia, and the generation of toxic oxygen radicals.

Published by Elsevier Inc.

Introduction

As the sophistication of enemy armed forces has increased, the United States and its allies have pursued more advanced armor and munitions. Although depleted uranium (DU) is considered very effective as an anti-armor ballistic material, significant controversy over the environmental and public health impact of its use in the Gulf War and the war in the Balkans has prompted the investigation and use of other materials including heavy metal tungsten alloys (HMTAs) as nontoxic alternatives (Miller and McClain, 2007; Monleau et al., 2006; van der Voet et al., 2007).

HMTAs are a category of tungsten-based substances containing 90 to 98% by weight tungsten (W) in combination with nickel (Ni), iron (Fe), copper, and/or cobalt (Co) (van der Voet et al., 2007). Due to their impressive ballistic properties (high density, strength, and stiffness) and a belief that tungsten and its alloys were relatively inert (based on studies investigating pure tungsten or tungsten carbide), HMTAs have been the leading candidates to replace DU and lead in military munitions (Gold et al., 2007; van der Voet et al., 2007). Discovery of the superior mechanical properties obtained from the W–Ni–Co and W–Ni–Fe alloy systems has led to their recent use and development for fragmentation warheads and kinetic energy penetrators for defeating heavy armor (Gold et al., 2007; van der Voet et al., 2007). Kinetic energy penetrators are armor-piercing weapons which do not contain explosives but use kinetic energy to penetrate the target; therefore they are made from the densest metals available. Because of the manufacturing process and the high melting temperature of W, HMTAs are actually a heterogeneous

Abbreviations: BAL, bronchoalveolar lavage; Cdkn1a, cyclin-dependent kinase inhibitor 1A; CINC, cytokine-induced neutrophil chemoattractant; CYP2A3, cytochrome P450, family 2, subfamily A, polypeptide 3; DCF, 2′,7′-dichlorodihydrofluorescein; DCFH-DA, 2′,7′-dichlorodihydrofluorescin diacetate; DU, depleted uranium; HMTA, heavy metal tungsten alloy; IL, interleukin; LDH, lactate dehydrogenase; Nos2/iNOS, nitric oxide synthase 2, inducible; ROS, reactive oxygen species; RNS, reactive nitrogen species; TNF-α, tumor necrosis factor alpha; WNiCo, reconstituted mixture of tungsten (W), nickel (Ni), and cobalt (Co); WNiFe, reconstituted mixture of tungsten (W), nickel (Ni), and iron (Fe).

☆ The views expressed herein are those of the authors and do not reflect the official policy or position of the Department of the Army, the Department of Defense, or the US Government.

* Corresponding author at: Department of Clinical Investigation, Tripler Army Medical Center, 1 Jarrett White Road, Honolulu, HI 96859, USA. Fax: +1 808 433 7160.
E-mail addresses: Erik.Roedel@amedd.army.mil (E.Q. Roedel), Danielle.Cafasso@amedd.army.mil (D.E. Cafasso), Karen.W.Lee@amedd.army.mil (K.W.M. Lee), Lisa.Pierce@amedd.army.mil (L.M. Pierce).

0041-008X/$ – see front matter. Published by Elsevier Inc.
doi:10.1016/j.taap.2011.12.008

mixture of pure W particles (tungsten phase) embedded in a matrix that is a true alloy (binder phase) made up of a small amount of dissolved W and alloying elements such as Ni, Co, and Fe (Harris et al., 2011; Kalinich et al., 2008; Machado et al., 2010, 2011). The binder phase corrodes more rapidly than the tungsten phase, releasing the alloying elements into solution (Kalinich et al., 2008; Ogundipe et al., 2006).

Interest in the health effects of HMTAs has peaked since the recent discovery that rats intramuscularly implanted with pellets containing 91.1% W, 6% Ni, and 2.9% Co rapidly developed aggressive metastatic tumors at the implantation site (Kalinich et al., 2005). This unanticipated finding raised extreme concern over the potential health effects of HMTA-based munitions, and, as a result, long-term exposure from internalized retained HMTA fragments has been a major focus of attention by the military medical community (Kalinich et al., 2008; Kane et al., 2009; van der Voet et al., 2007). The *in vivo* carcinogenic potential of HMTAs containing W, Ni, and Co is supported by *in vitro* studies which demonstrated that exposure to military-relevant mixtures of W, Ni, and Co (WNiCo) induced malignant transformation, generation of reactive oxygen species (ROS), oxidative DNA damage, and expression of several stress genes in various cultured cell types, suggesting a synergistic effect that exceeded the effects of the metals individually (Harris et al., 2011; Miller et al., 2002, 2004). Although military-relevant mixtures of W, Ni, and Fe (WNiFe) also induced genotoxic effects and induced cell transformation *in vitro* (Miller et al., 2001), other studies found that WNiFe was less toxic than WNiCo and did not induce tumors in rats (Harris et al., 2011; Kalinich et al., 2005; Roszell et al., 2008).

In addition to risks associated with HMTAs after internalization as retained fragments, military personnel may be at risk of respiratory tract injury after acute exposure to aerosolized HMTA particles generated at high temperature when tungsten alloy munitions strike hard targets (Gold et al., 2007; Machado et al., 2010, 2011). The Capstone DU Aerosol Characterization and Risk Assessment Study was conducted initially to assess inhalation exposure to DU aerosols and risk to soldiers in combat vehicles and to first responders at the time of perforation by a DU penetrator (Parkhurst and Guilmette, 2009). The predicted median inhalation intakes of DU from the generated aerosols ranged from a low of 10 mg for a 1-minute exposure in a ventilated Abrams tank with DU armor to a high of 710 mg for a 5-minute exposure in an unventilated Abrams tank with DU armor. Gold et al. (2007) conducted a quantitative analysis of aerosols generated inside of an armored vehicle perforated by a kinetic energy penetrator containing W, Ni, and Co. They showed that respirable particles (<10 μm) were generated at doses twice the concentration listed as immediately dangerous to life or health by the National Institute for Occupational Safety and Health. More recently, Machado et al. (2010, 2011) characterized the size distribution and composition of particulates created by W–Ni–Co and W–Ni–Fe penetrator rods perforating a series of steel target plates and determined the relative fractions of Co, Ni, W, and Fe. Particulates collected on individual filters were discovered to be highly toxic to human lung epithelial cells, suggesting severe human toxicity potential for inhaled ballistic aerosolized metals (Machado et al., 2010, 2011).

Despite these concerns, pulmonary toxicity caused by HMTA-based metallic particles has never been investigated *in vivo*, and very little is known concerning the molecular mechanisms leading to the pathological effects associated with inhalation exposure to HMTAs. In the present study we wished to determine whether *in vivo* exposure to military-relevant reconstituted HMTA mixtures of W, Ni, and Co (WNiCo) or W, Ni, and Fe (WNiFe) induces pulmonary inflammation and altered expression of genes associated with oxidative and metabolic stress and toxicity in the rat. We also wished to determine the effects of *in vitro* exposure on two parameters of lung macrophage function, the oxidative burst response and phagocytosis.

Material and methods

Metal powders. The weight percentage composition of HMTAs containing W/Ni/Co or W/Ni/Fe currently used in military munitions is approximately 91–93% W, 3–5% Ni, and either 2–4% Co or 2–4% Fe (Miller et al., 2001; van der Voet et al., 2007). Because HMTAs used by the military are not commercially available, we used a mixture of these metals, in the same percentages used by the military, to model the particles of the alloy similar to the methods of Miller et al. (2001). Metals were obtained from Alfa Aesar (Ward Hill, MA) and included tungsten powder (W; Alfa Aesar 10400, 99.9% purity, median particle size 1–5 μm), nickel powder (Ni; Alfa Aesar 10256, 99.9% purity, median particle size 3–7 μm), cobalt powder (Co; Alfa Aesar 10455, 99.8% purity, median particle size 1.6 μm), and iron powder (Fe; Alfa Aesar 00170, 99.9% purity, median particle size <10 μm). The alloys tested in this study (WNiCo and WNiFe) consisted of a pure mixture of insoluble W (92%), Ni (5%), and either Co (3%) or Fe (3%) particles made in the laboratory. Dose–response experiments were conducted by altering the amounts of each metal powder, based upon its percentage of 100% of the total amount of powders. For example, 1 mg WNiCo was composed of 0.92 mg W, 0.05 mg Ni, and 0.03 mg Co, while 2 mg WNiCo consisted of 1.84 mg W, 0.1 mg Ni, and 0.06 mg Co. Thus the total amount (weight) of the metal powder mixture was varied while the ratio of the component metals was held constant. Effects of individual metals were also examined according to their percentages in the WNiCo and WNiFe mixtures. For *in vivo* studies, insoluble metal particles were suspended in sterile saline and agitated immediately prior to intratracheal instillation. For *in vitro* studies, particles were suspended in acetone and vortexed immediately before being dispensed into cell cultures.

Animals. Adult male Sprague–Dawley rats (9 weeks of age, approximately 300 g) were obtained from Taconic (Germantown, NY) and housed in polycarbonate cages in HEPA-filtered laminar airflow racks with wood chip bedding under controlled lighting conditions (12 h light/12 h dark). The rats were allowed free access to standard laboratory diet and tap water. The study protocol was approved by the Institutional Animal Care and Use Committee at Tripler Army Medical Center. Investigators complied with the policies as prescribed in the USDA Animal Welfare Act and the National Research Council's "Guide for the Care and Use of Laboratory Animals." Facilities are fully accredited by the Association for Assessment and Accreditation of Laboratory Animal Care International. Each experiment or assay was performed using 3–6 different rats per treatment group.

Intratracheal instillation. Rats were lightly anesthetized by an intraperitoneal (ip) injection of sodium pentobarbital (20 mg/kg) and/or isoflurane (2–5%). Animals were intratracheally instilled with WNiCo or WNiFe (1, 2, and 4 mg/100 g body weight) or individual metals in an instillation volume of 1 ml/kg body weight sterile saline suspension using a 16-gauge catheter (1.7×50 mm, B. Braun Medical, Inc., Bethlehem, PA) according to the method of Brain et al. (1976). Rats in the vehicle control group were instilled with 1 ml/kg body weight sterile saline. Doses chosen for this study were adapted from those used in *in vivo* studies of hard metal alloys consisting of tungsten carbide and Co particles and fell within the range of doses that induced acute pulmonary toxicity (De Boeck et al., 2003; Huaux et al., 1995; Lison and Lauwerys, 1994). Because this study focused on the effects of acute exposure, all rats were allowed to recover for 24 h before subsequent experiments were performed.

Bronchoalveolar lavage (BAL) and cell differentials for measurement of pulmonary inflammation. Twenty-four hours after intratracheal instillation, rats were euthanized with sodium pentobarbital (150 mg/kg, ip). A 16 gauge catheter was inserted into the trachea through a cut

in the cricoid membrane, and BAL (6 ml per lavage) was performed through the catheter using ice-cold Dulbecco's Ca^{2+}/Mg^{2+}-free phosphate-buffered saline (DPBS, Sigma Aldrich, St. Louis, MO). The first lavage was kept separate from the remainder of the lavage sample. Subsequent lavages were pooled and kept on ice until a total of 50 ml BAL fluid was collected. Samples were centrifuged (216×*g*, 10 min at 4 °C), and the acellular first lavage supernatant was stored at −70 °C for microplate-based assays to determine lactate dehydrogenase (LDH) activity, albumin content, and inflammatory cytokine levels. Cells were combined, resuspended in 10 ml DPBS, and counted using a Vi-Cell XR Cell Viability Analyzer (Beckman Coulter, Inc., Brea, CA). Cells were then centrifuged a second time and resuspended at a final concentration of 1×10^8 live cells/ml. Microscope slide smears were prepared using 5 μl of the cell suspension (4–6 slides per animal). Microscope slide smear preparation has been shown to be a simple and accurate method for the quantitation of BAL fluid cytology (Thompson et al., 1996). Percentages of neutrophils were determined by examination of Wright-Giemsa (Polysciences, Inc., Warrington, PA)-stained slides. A minimum of 300 cells per animal were differentially counted. Metal particles were observed in BAL samples from all animals used in analysis except vehicle (sterile saline) controls.

BAL fluid LDH activity and albumin concentration. BAL fluid LDH activity was determined as a marker of cytotoxicity induced by the instilled particles and was measured by monitoring the LDH-catalyzed oxidation of pyruvate coupled with the reduction of nicotinamide adenine dinucleotide at 490 nm using a commercially available LDH Cytotoxicity Assay Kit (Cayman Chemical Company, Ann Arbor, MI) and a SpectraMax M2 multi-mode plate reader (Molecular Devices, Inc., Sunnyvale, CA) according to the manufacturer's instructions. To examine whether instilled particles compromised the integrity of the blood-pulmonary epithelial cell barrier, albumin concentrations in the BAL fluid were determined using the Albumin Blue Fluorescent Assay Kit (Active Motif, Carlsbad, CA) following the manufacturer's protocol and measuring fluorescence (excitation 560 nm, emission 620 nm) on the microplate reader. The detection limit of this assay was 0.5 μg/ml. All assays were performed in duplicate or triplicate wells.

Measurement of proinflammatory cytokines in BAL fluid. The quantity of rat cytokine-induced neutrophil chemoattractant-1 (CINC-1) and rat CINC-3, the combined functional homologs to human interleukin 8 (IL-8) (Mukaida, 2003), as well as tumor necrosis factor alpha (TNF-α) and interleukin 1 beta (IL-1β), was determined by enzyme-linked immunosorbent assay kits (R&D Systems, Minneapolis, MN) according to the manufacturer's protocols. The detection limit was 1.3 pg/ml for CINC-1, 2.7 pg/ml for CINC-3, 5 pg/ml for TNF-α, and 5 pg/ml for IL-1β. All assays were performed in duplicate or triplicate wells.

Lung histology. After lavage, lungs were instilled with 8 ml 10% neutral buffered formalin to achieve full expansion of the different lobes and were fixed in formalin for at least 24 h. Slices from all lung lobes were embedded in paraffin and 5 μm sections (8 sections per lung lobe per animal) were cut and stained with hematoxylin–eosin. Pulmonary inflammation was evaluated qualitatively in animals instilled with WNiCo and WNiFe (1, 2 and 4 mg/100 g body weight), W (0.92, 1.84, and 3.68 mg/100 g body weight), Ni (0.10 mg/100 g body weight), Co (0.06 mg/100 g body weight), Fe (0.06 mg/100 g body weight), and saline by light microscopy. Digital images were captured using PictureFrame software (Optronics, Goleta, CA) and an Olympus IX71 microscope (Olympus America, Inc., Center Valley, PA).

Immunohistochemistry. Immunohistochemistry was performed on 5 μm paraffin sections of lung tissue using an anti-CYP2A rabbit polyclonal antibody (H-110, sc-33214; Santa Cruz Biotechnology, Inc., Santa Cruz, CA) to confirm CYP2A3 expression patterns identified in the WNiCo gene expression profiles for whole lung. Because a specific antibody for rat CYP2A3 was not commercially available, we used this antibody, which detects a broad range of CYP2A family members of rat and human origin, with the understanding that CYP2A3 is the principal P450 2A enzyme expressed in the rat lung (Ling et al., 2004). After deparaffinization and rehydration, microwave antigen retrieval with citrate buffer (Millipore, Temecula, CA) was performed, and immunostaining occurred with the use of the Dako EnVision System (Dako North America Inc., Carpinteria, CA) following the manufacturer's instructions. Briefly, sections were incubated with an endogenous enzyme block solution for 5 min, rinsed twice in wash buffer for 5 min each, incubated with an endogenous rat immunoglobulin blocking reagent (Rodent Block R; Biocare Medical, Concord, CA) for 25 min, and incubated for 15 min at room temperature with the CYP2A antibody applied at a dilution of 1:50. Sections were rinsed and incubated for 25 min with a dextran polymer conjugated with horseradish peroxidase and affinity-isolated immunoglobulins containing the blocking reagent XR Factor (Biocare Medical). Rinsed sections were then incubated for 10 min with a 3,3′-diaminobenzidine chromogen-substrate to form a colored reaction product. Slides were counterstained with Mayer's hematoxylin (Dako North America, Inc.), dehydrated, and permanently mounted. Negative controls were achieved by omission of the primary antibody or by applying a rabbit universal negative control reagent (Dako North America, Inc.) instead of the rabbit polyclonal primary antibody.

Degree of positive immunostaining was scored on a scale of 0–4 (0 = none, 1 = minimal, 2 = mild, 3 = moderate, 4 = intense). A total of 4–8 sections per animal (2–4 lung lobes per animal, 2 sections per lobe) were examined in 4 rats instilled with 2 mg WNiCo/100 g body weight and 4 rats instilled with saline, and average scores were calculated. For WNiCo-exposed rats, lung sections were required to demonstrate the presence of metal particles to be included in analysis, and thus the scorer was necessarily not blinded to exposure.

Gene expression profiling in BAL cells and in whole lung. To determine the effects of alloy or individual metals on gene expression in BAL cells at a dose which induced only mild pulmonary toxicity *in vivo*, rats were intratracheally instilled with 2 mg WNiCo/100 g body weight, 2 mg WNiFe/100 g body weight, equivalent amount of individual metals used in the tungsten alloys, or saline. BAL cells were collected as described above, and total RNA was purified from cell pellets according to the instructions provided in the RNeasy Mini Kit (Qiagen, Valencia, CA). RNA was quantified using a spectrophotometer (Cary 50, Varian, Inc, Palo Alto, CA) and then stored at −70 °C. Complementary DNA was generated from 1 μg total RNA using the RT^2 First Strand Kit (Qiagen) and analyzed using a Rat Stress and Toxicity PathwayFinder RT^2 Profiler PCR Array (Qiagen) by means of a Bio-Rad iCycler real-time PCR Detection System (Bio-Rad Laboratories, Hercules, CA) according to the manufacturer's instructions. This array is a set of optimized real-time PCR primer assays (specific for rat samples) on 96-well plates for pathway-focused genes as well as appropriate RNA quality controls and internal control housekeeping genes to normalize the data for the amount of RNA added to each reverse transcription reaction. The Rat Stress and Toxicity PathwayFinder RT^2 Profiler PCR Array profiles the expression of 84 genes whose expression level is indicative of stress and toxicity, including those involved in oxidative or metabolic stress, DNA damage and repair, proliferation and carcinogenesis, inflammation, heat shock, and apoptosis. A complete list of genes contained in the array can be viewed on the following link: http://www.sabiosciences.com/rt_pcr_product/HTML/PARN-003A.html. Arrays were repeated with 3–5 different rats in each experimental group using total RNA isolated from a single rat per array.

To determine the effects of alloy or individual metals on gene expression in whole lung tissue at a dose which induced only mild

pulmonary toxicity *in vivo*, additional rats were intratracheally instilled with 2 mg WNiCo/100 g body weight, corresponding doses of individual metals, or saline. Non-lavaged lungs were harvested 24 h after instillation and were stored in RNALater (Ambion Inc, Austin, TX) at −20 °C until RNA isolation was performed. Samples were homogenized using an Omni GLH homogenizer (Omni International, Kennesaw, GA), and total RNA was isolated using the Trizol method according to the manufacturer's instructions (Invitrogen, Carlsbad, CA). Extracted RNA was further purified using the RNeasy Mini Kit (Qiagen), quantified using a spectrophotometer, and then stored at −70 °C. Arrays were run as described above using total RNA isolated from a single rat per array (5 arrays per experimental group).

In vitro cytotoxicity assays. Cell viability was analyzed using alamarBlue Cell Viability Reagent (Invitrogen, Carlsbad, CA) which measures the metabolic capacity of cells to reduce resazurin to resorufin, a highly fluorescent compound. Cells were collected by BAL from untreated rats as described, which contain >95% lung macrophages (Pierce et al., 1996). Cells (5×10^5/ml) were suspended in RPMI 1640/0.05% bovine serum albumin (Sigma-Aldrich Co., St. Louis, MO) and 50,000 cells/well (100 μl) were plated in 96-well black tissue culture plates (Santa Cruz Biotechnology, Inc.). Metal particles suspended in acetone were vortexed immediately before being added to wells at a final concentration of 12.5, 25, 50, 100, 200, 400, and 1000 μg/ml (WNiCo and WNiFe), or equivalent amount of individual metals W, Ni, and Co or Fe used in the tungsten alloys. The alamarBlue reagent was then added to wells (10 μl) and cells were incubated for 4 h at 37 °C/5% CO_2 based upon the manufacturer's recommendations. Fluorescence was measured (excitation 560 nm, emission 590 nm) on the SpectraMax M2 multi-mode plate reader (Molecular Devices, Inc.). The average background fluorescence values of the cell culture medium plus metals alone were subtracted from the fluorescence values of experimental wells. Data were normalized to values obtained for untreated cells plus acetone. Assays were performed in triplicate wells and included determinations from 3 separate experiments.

Oxidative burst assays. Intracellular reactive oxygen species (ROS) and reactive nitrogen species (RNS) generation by lung macrophages was measured using the OxiSelect Intracellular ROS Assay Kit (Cell Biolabs, Inc., San Diego, CA). The assay uses the cell permeable fluorogenic probe 2′,7′-dichlorodihydrofluorescin diacetate (DCFH-DA), which diffuses into cells and is deacetylated by cellular esterases to non-fluorescent DCFH. In this reactive state, ROS and RNS including hydrogen peroxide, peroxyl radical, nitric oxide, and peroxynitrite anion can react with DCFH, which is rapidly oxidized to the highly fluorescent 2′,7′-dichlorodihydrofluorescein (DCF). Fluorescence intensity is proportional to the total ROS/RNS levels within the cell cytosol.

Cells were collected by BAL from untreated rats as described, suspended (5×10^5/ml) in Hank's Balanced Salt Solution (Sigma-Aldrich Co.), and incubated 2 h at 37 °C/5% CO_2 in 96-well black culture plates (50,000 cells/well). DCFH-DA was then added to each well at a final concentration of 1 mM and incubated for 30 min at 37 °C/5%CO_2. At this time metal suspensions were added to experimental wells as described for *in vitro* cytotoxicity assays at final concentrations of 12.5, 25, 50, 100, and 200 μg/ml (WNiCo and WNiFe), or equivalent amount of individual metals W, Ni, and Co or Fe used in the tungsten alloys, and plates were incubated for 1 h at 37 °C/5% CO_2. An incubation time of one hour was chosen because preliminary studies determined that the oxidative burst response peaks at 1–2 h, while the background fluorescence elicited by the metals in the serum-free media is negligible at this time point. Fluorescence was measured at 480 nm excitation/530 nm emission in the fluorescence microplate reader. Data were normalized to values obtained for untreated cells plus acetone. Assays were performed in triplicate wells and included determinations from 4 separate experiments.

Phagocytosis assays. Phagocytosis by lung macrophages was measured using the CytoSelect 96-Well Phagocytosis Assay (Zymosan; Cell Biolabs, Inc.) according to the manufacturer's instructions. This assay uses prelabeled zymosan particles prepared from the yeast cell wall as a phagocytosis pathogen. External zymosan particles are blocked before the colorimetric detection of engulfed particles, enabling a quantitative, high-throughput method to detect phagocytosis in a 96-well format.

Briefly, cells were collected by BAL from untreated rats as described, suspended (1×10^6/ml) in RPMI 1640/0.05% bovine serum albumin, and 100,000 cells/well (100 μl) were plated in 96-well tissue culture plates (Santa Cruz Biotechnology, Inc.). Metal particles were added to wells at a final concentration of 0, 25, 50, 100, and 200 μg/ml (WNiCo and WNiFe), and cells were incubated for 30 min at 37 °C/5% CO_2 (per previously established protocol for this assay in our laboratory). The nonopsonized zymosan suspension was then added to wells (10 μl), mixed well, and cells were incubated for an additional 1.5 h at 37 °C/5% CO_2. A series of washing, fixation, blocking, permeabilization, and detection steps was then performed as recommended by the manufacturer, and the absorbance of each well was read at 405 nm in the microplate reader. Each sample, including a negative control without zymosan particles, was assayed in triplicate wells and determinations from 4 separate experiments were included in analysis.

Statistical analysis. All results are reported as means ± standard error of the mean (SEM). Changes in gene expression analyzed using the RT^2 Profiler PCR Array were calculated using software from Qiagen. Differentially expressed genes were considered significant using a cutoff value >3-fold change and $p<0.05$. Differences between vehicle-treated animals and those exposed to WNiCo, WNiFe, or individual metals were evaluated using one-way analysis of variance (ANOVA) followed when appropriate using a multiple comparison test (Holm–Sidak method). Comparisons between groups were also performed using the Student t test. Corresponding nonparametric tests were used when appropriate. Statistical analyses were performed using SigmaPlot 11.2 software (Systat Software, Inc., San Jose, CA), with $p<0.05$ considered significant.

Results

WNiCo and WNiFe particles induce pulmonary inflammation in vivo in a dose–response manner

Exposure to WNiCo and WNiFe particles had a significant dose–response effect on markers of acute inflammation and toxicity in BAL samples 24 h after instillation (Fig. 1). For WNiCo, percentage of neutrophils ($p<0.001$), CINC-1 ($p=0.005$), CINC-3 ($p=0.005$), IL-1β ($p=0.009$), and LDH activity ($p=0.03$) increased significantly with increasing dose. For WNiFe, percentage of neutrophils ($p<0.001$), CINC-1 ($p=0.001$), CINC-3 ($p=0.002$), TNF-α ($p<0.001$), IL-1β ($p<0.001$), and albumin ($p=0.004$) increased significantly with increasing dose. In general, for both WNiCo and WNiFe, 1 mg/100 g body weight elicited minimal effects, 2 mg/100 g body weight induced mild toxicity (indicated by neutrophil influx, increased albumin content, but no significant elevation in LDH activity), and 4 mg/100 g body weight induced moderate toxicity (indicated by a marked neutrophilia, increased inflammatory cytokine levels and albumin content, and a trend toward elevated LDH activity). The neutrophil influx observed in response to WNiCo and WNiFe was associated with a corresponding decrease in the percentage of macrophages ($p<0.001$, not shown) for both alloys and a small but significant elevation in the percentage of lymphocytes for WNiCo only (comprising up to 4% of the BAL cell population,

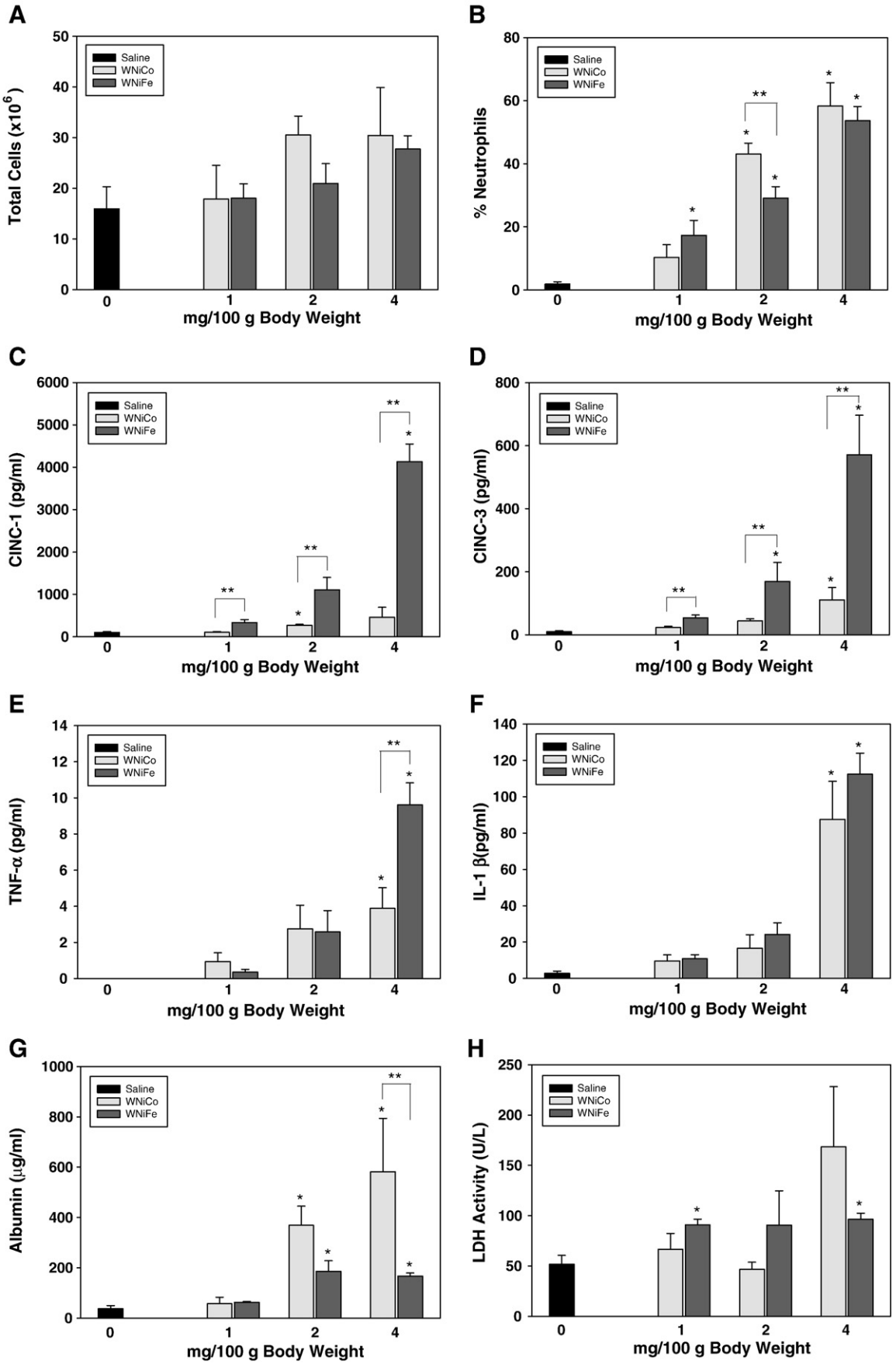

Fig. 1. Dose–response effect of WNiCo and WNiFe on markers of acute inflammation and toxicity in BAL samples measured 24 h after intratracheal instillation. The effects of 0 (saline), 1, 2, and 4 mg WNiCo or WNiFe/100 g body weight on (A) total cells, (B) percentage neutrophils, (C) CINC-1, (D) CINC-3, (E) TNF-α, (F) IL-1β, (G), albumin, and (H) LDH activity were evaluated. For each determination, n = 4–6. *$p<0.05$ compared to saline; ANOVA followed by multiple comparisons vs. saline using the Holm–Sidak method. **$p<0.05$, WNiCo vs. WNiFe; Student t test.

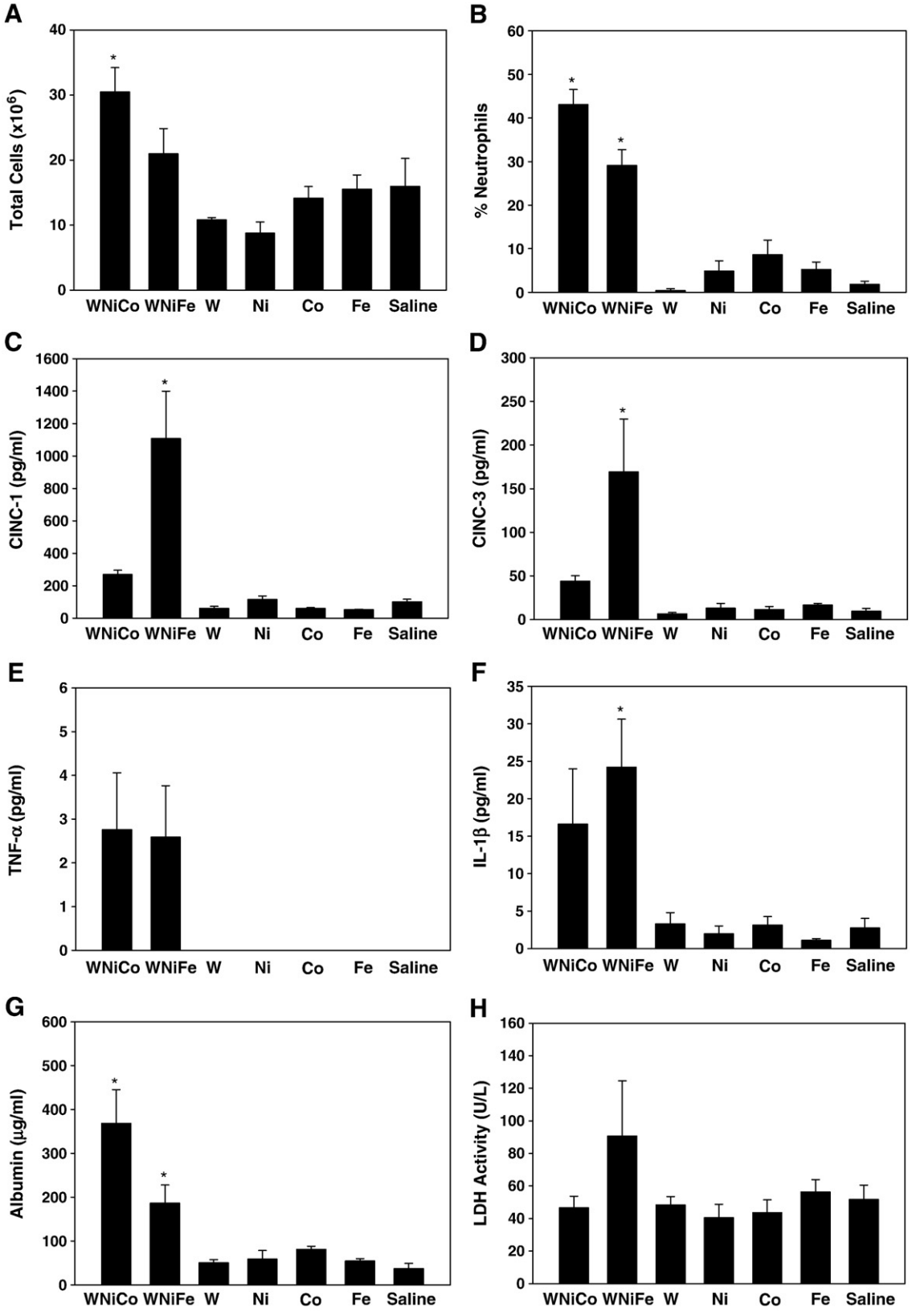

Fig. 2. Comparison of WNiCo, WNiFe, and individual metals on markers of acute inflammation and toxicity in BAL samples measured 24 h after intratracheal instillation. The effect of 2 mg WNiCo/100 g body weight, 2 mg WNiFe/100 g body weight, and equivalent amount of W, Ni, Co, and Fe used in the tungsten alloys on (A) total cells, (B) percentage neutrophils, (C) CINC-1, (D) CINC-3, (E) TNF-α, (F) IL-1β, (G), albumin, and (H) LDH activity were evaluated. For each determination, n = 3–6. *$p<0.05$ compared to saline; ANOVA followed by multiple comparisons vs. saline using the Holm–Sidak method.

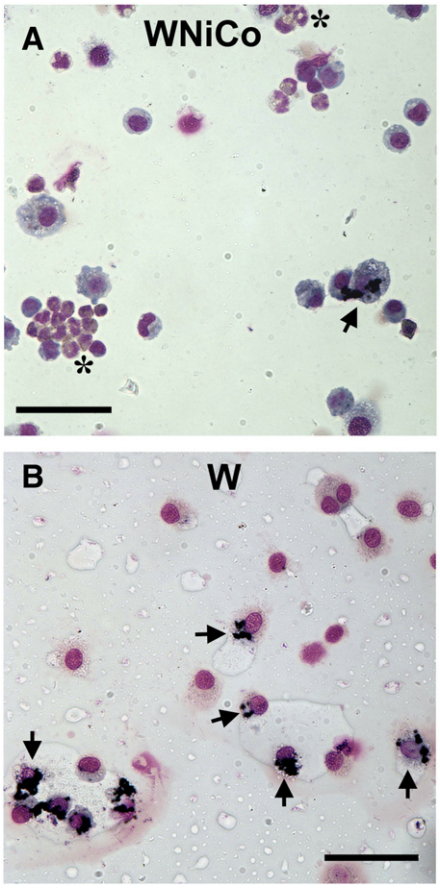

Fig. 3. Representative images of BAL cells 24 h after intratracheal instillation of (A) WNiCo (2 mg/100 g body weight) or (B) W (1.84 mg/100 g body weight). Note phagocytosis of metal particles by alveolar macrophages (arrows) in panels A and B and the influx of neutrophils (*) following the intratracheal instillation of WNiCo but not W. BAL cytology was similar between WNiFe and WNiCo (not shown). Original magnification ×640, bar = 50 μm.

$p<0.001$, not shown). The dose-dependent toxic effects of WNiCo and WNiFe were also reflected in a decrease in body weight 24 h after intratracheal instillation compared to saline-instilled animals. A significant decrease in body weight ($p<0.001$) was observed after exposure to WNiCo (2 mg/100 g body weight and 4 mg/100 g body weight) and WNiFe (4 mg/100 g body weight), but not after exposure to the individual metals ($p>0.05$).

In contrast, the instillation of pure tungsten at doses of 0.92, 1.84, and 3.68 mg W/100 g body weight resulted in no significant change in any of the markers of inflammation or toxicity examined in BAL fluid until the highest dose was reached (not shown). At this dose, signs of mild inflammation were evident (neutrophils made up 30% of the BAL cell population and albumin content was mildly elevated at 277 ± 27 μg/ml), although there was no elevation of inflammatory cytokines or other markers including LDH activity or a change in body weight to indicate any significant toxicity elicited by pure tungsten.

WNiCo was more toxic than WNiFe, as indicated by the higher albumin content and trend toward elevated LDH activity in the BAL fluid from WNiCo-exposed animals (Fig. 1). Although the neutrophil influx increased similarly for both HMTAs (nearly 60% of the BAL cell population at the 4 mg/100 body weight dose), greater levels of the neutrophil chemoattractants CINC-1 and CINC-3 in BAL fluid were observed in WNiFe-exposed animals compared to WNiCo at all three concentrations evaluated (Fig. 1). IL-1β protein levels were significantly elevated at the highest dose for both WNiFe and WNiCo, while TNF-α protein levels in BAL fluid were low but greater for WNiFe than WNiCo at the highest dose.

The contribution of individual metals was then compared to the effects elicited by the two HMTAs investigated in this study at a dose which induced mild pulmonary toxicity (2 mg WNiCo or WNiFe/100 g body weight). WNiCo, but not the equivalent amount of W, Ni, and Co used in the alloy (1.84, 0.10, and 0.06 mg/100 g body weight, respectively) induced a significant increase in total cells, percentage neutrophils, and albumin content in BAL fluid compared to rats instilled with saline (Figs. 2 and 3). WNiFe, but not the equivalent amount of W, Ni, and Fe used in the alloy (1.84, 0.10, and 0.06 mg/100 g body weight, respectively), induced a significant increase in percentage neutrophils, inflammatory cytokines CINC-1, CINC-3, and IL-1β, and albumin content in BAL fluid compared to animals instilled with saline (Fig. 2).

The quantitative analysis of BAL fluid was reflected qualitatively in histologic sections of lung tissue evaluated from rats instilled with saline, WNiCo, WNiFe, and individual metals (Fig. 4). Elevated numbers of inflammatory cells were observed in WNiCo- and WNiFe-exposed lungs compared to those instilled with saline or individual metals, and inflammatory cells and associated metal particles were more prevalent with increased dose (Fig. 4). Phagocytosis of metal particles, which occurred predominantly in alveolar macrophages, was evident in BAL cytological specimens and in tissue sections (Figs. 3 and 4).

Effect of in vivo WNiCo and WNiFe exposure on gene expression in BAL cells

Expression profiling of stress and toxicity genes was performed in BAL cells to determine whether *in vivo* exposure to WNiCo (2 mg/100 g body weight), WNiFe (2 mg/100 g body weight), or equivalent amount of individual metals used in the alloys alters gene expression 24 h after intratracheal instillation. Using a cutoff value of >3 fold change compared to saline-instilled animals and $p<0.05$, 14 genes were differentially expressed in response to WNiCo, 17 genes were differentially expressed in response to WNiFe, and 10 genes overlapped between the two alloys which were primarily involved in inflammation and growth arrest and senescence (Table 1). In contrast, 2 genes were differentially expressed in response to W, 3 genes were differentially expressed in response to Ni, one gene was differentially expressed in response to Co, and no genes were differentially expressed in response to Fe (not shown). Genes most markedly induced in BAL cells after WNiCo exposure relative to saline controls included inducible nitric oxide synthase (Nos2/iNOS; 49-fold increase, $p<0.001$) and IL-6 (34-fold increase, $p=0.03$). These mRNA expression levels greatly exceeded those from animals instilled with the individual metals, suggesting a synergistic effect (not shown). Although IL-6 was also markedly elevated after exposure to WNiFe (26-fold increase, $p<0.001$), Nos2/iNOS mRNA levels were lower in response to WNiFe (14-fold increase relative to saline-instilled animals, $p<0.03$) compared to WNiCo. In addition, WNiFe induced a greater heat shock response in BAL cells than WNiCo (4 genes encoding heat shock proteins were elevated after WNiFe exposure compared to one gene after WNiCo exposure) and induced the downregulation of two genes involved in DNA damage and repair (Table 1).

Effect of in vivo WNiCo exposure on gene expression in whole lung tissue

Gene expression profiling was performed in non-lavaged whole lung tissue to determine whether *in vivo* exposure to WNiCo at a dose which produces only mild toxicity (2 mg/100 g body weight) induces the expression of genes associated with stress and toxicity 24 h after intratracheal instillation. Of the 84 genes examined in the Rat Stress and Toxicity PathwayFinder RT^2 Profiler PCR Array, only 2 genes were detected as being differentially expressed (>3-fold change, $p<0.05$) in whole lung relative to saline (Fig. 5). These included genes which encode the inflammatory cytokine IL-6 and

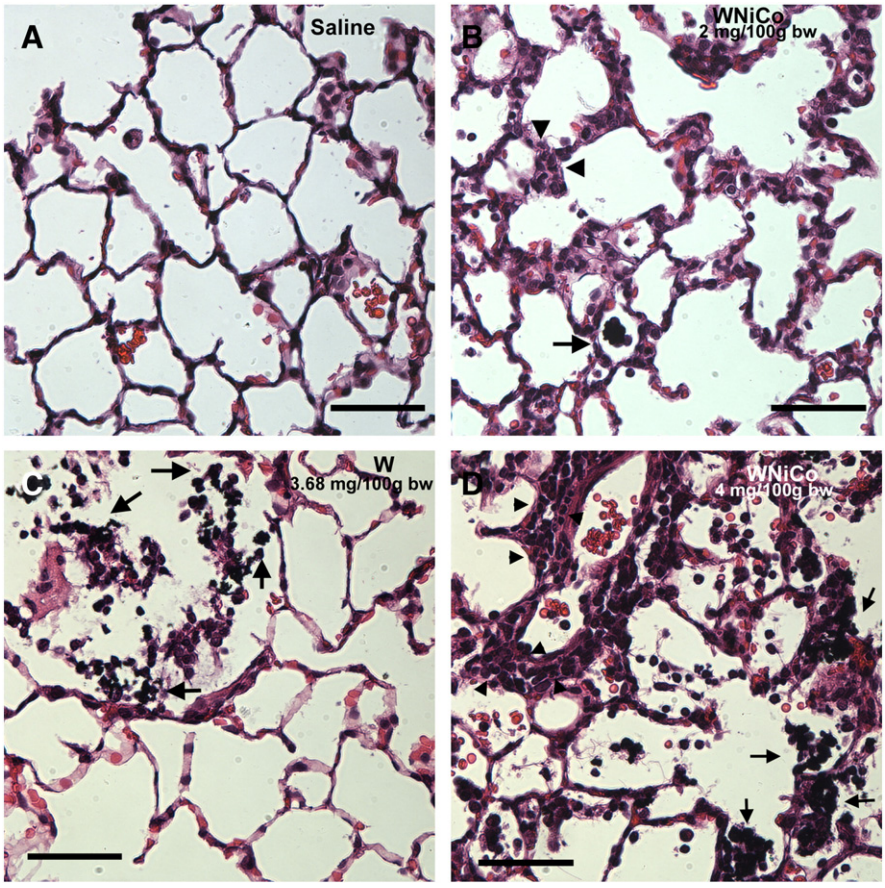

Fig. 4. Histologic evidence of pulmonary inflammation 24 h after intratracheal instillation of WNiCo. Representative lung sections stained with hematoxylin and eosin from animals instilled with (A) saline (vehicle), (B) WNiCo (2 mg/100 g body weight), (C) W (3.68 mg/100 g body weight), and (D) WNiCo (4 mg/100 g body weight). Arrows denote agglomerated W or WNiCo particles in an alveolar space associated with alveolar macrophages. Arrowheads indicate neutrophils located in the interstitium. Note elevated numbers of inflammatory cells in WNiCo-exposed lungs relative to those instilled with saline and W. Original magnification ×640, bar = 50 μm. Results were similar between WNiFe and WNiCo (not shown).

CYP2A3, an important cytochrome p450 enzyme preferentially expressed in the respiratory tract which is the rat ortholog of human CYP2A13 (Ling et al., 2004). The instillation of WNiCo induced a remarkable 42-fold decrease in CYP2A3 mRNA expression ($p = 0.001$) and a 7-fold increase in IL-6 mRNA expression ($p = 0.04$) relative to animals instilled with saline (Fig. 5). The reduced CYP2A3 expression in WNiCo-exposed animals relative to saline controls was confirmed at a protein level in sections of lung

Table 1
Differentially expressed stress and toxicity-related genes in BAL cells 24 h after intratracheal instillation of 2 mg WNiCo/100 g body weight (n = 3) or 2 mg WNiFe/100 g body weight (n = 5). Data represent mean fold change compared to rats instilled with saline (n = 5). A complete list of genes and their descriptions contained in the array can be viewed on the following link: http://www.sabiosciences.com/rt_pcr_product/HTML/PARN-003A.html. Genes with > 3-fold change and $p < 0.05$ are highlighted in bold.

Functional grouping	Gene	Fold change WNiCo	p	Fold change WNiFe	p
Apoptosis signaling	Nfkbia (ikBa/Mad3)	**3.30**	**<0.001**	1.36	0.10
	Casp1 (ICE)	**−3.07**	**0.01**	−1.37	0.05
DNA damage and repair	Chek2	−1.93	0.01	**−3.52**	**<0.001**
	Ugt1a6	−1.54	0.26	**−5.26**	**0.005**
Growth arrest and senescence	Cdkn1a (p21Waf1/p21Cip1)	**5.83**	**<0.001**	**8.25**	**<0.001**
	Ddit3 (Gadd 153/CHOP)	**4.22**	**0.03**	**4.07**	**<0.001**
Heat shock	Hspa1a (Hsp70-1)	**16.49**	**<0.001**	**24.34**	**0.004**
	Hsph1 (Hsp105)	1.28	0.49	**4.74**	**0.01**
	Hspa8	−1.22	0.55	**3.40**	**<0.001**
	Hspb1 (Hsp25)	1.46	0.74	**13.78**	**0.02**
Inflammation	Ccl3 (MIP-1a)	**15.67**	**0.04**	**5.22**	**0.001**
	Ccl4 (MIP-1b)	**7.31**	**0.02**	4.74	0.07
	Csf2 (GM-CSF)	**16.95**	**<0.001**	**5.92**	**0.03**
	Il1b	**6.05**	**0.01**	**7.70**	**0.008**
	Il6	**33.90**	**0.03**	**25.72**	**<0.001**
	Lta (Tnfb)	**5.03**	**0.02**	**19.77**	**0.007**
	Mif	12.91	0.06	**7.81**	**<0.001**
	Nos2 (iNOS)	**49.07**	**<0.001**	**14.37**	**0.03**
	Il18	**−3.18**	**0.04**	−2.70	0.002
Oxidative or metabolic stress	Cyp4a14	−3.32	0.85	**−5.05**	**<0.001**
Proliferation and carcinogenesis	E2f1	**−3.41**	**0.002**	**−4.52**	**<0.001**

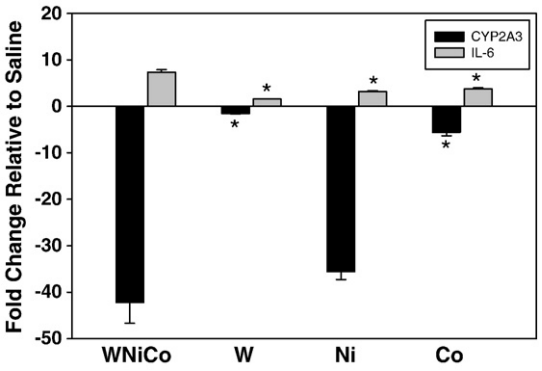

Fig. 5. Effect of WNiCo and individual metals on stress and toxicity-related gene expression in lung tissue 24 h after intratracheal instillation. Rats were exposed to 2 mg/100 g body weight WNiCo or equivalent amount of W, Ni, and Co used in the tungsten alloy ($n=5$ per group). Data represent mean ± SEM of WNiCo-, W-, Ni-, and Co-induced fold change compared to lungs from animals intratracheally instilled with vehicle (saline) only. Of the 84 genes examined in the Rat Stress and Toxicity PathwayFinder PCR Array, only CYP2A3 and IL-6 were differentially expressed (>3 fold change, $p<0.05$) in at least one of the individual metals or tungsten alloy investigated in this study. *$p<0.05$ compared to WNiCo; ANOVA followed by pairwise multiple comparisons using the Holm–Sidak method.

tissue stained with CYP2A antibodies, particularly in the bronchiolar epithelium (Fig. 6). Scores for CYP2A immunohistochemical staining intensity were significantly higher in saline-instilled lungs than those instilled with WNiCo (2.9 ± 0.2 vs. 1.6 ± 0.2, respectively, $p=0.004$). Although W exposure did not affect CYP2A3 or IL-6 mRNA expression, Ni demonstrated significant downregulation of CYP2A3 (36-fold decrease, $p=0.001$) and upregulation of IL-6 (3-fold increase, $p=0.04$), while Co showed a 6-fold decrease in CYP2A3 ($p=0.01$) and a 4-fold increase in IL-6 ($p=0.01$).

Dose-dependent cytotoxic effects of metal treatment on BAL cells in vitro

The toxic effects of WNiCo (12.5–1000 μg/ml), WNiFe (12.5–1000 μg/ml), and equivalent amount of the constituent metals used in the tungsten alloys were tested *in vitro* on rat BAL cells harvested from untreated animals. Tungsten and its alloys showed significant dose-dependent decreases in metabolic viability at 100 μg/ml, 200 μg/ml, 400 μg/ml, and 1000 μg/ml, but not at 50 μg/ml or below (Table 2). In contrast, Co and Fe at concentrations present in the alloys did not demonstrate significant toxicity (Table 2). Ni had no consistent significant effect on viability. The small amount of acetone used to suspend the metal particles had no detrimental effect on cell viability (not shown).

Intracellular ROS/RNS generation by lung macrophages collected by BAL

WNiCo ($p<0.001$) and WNiFe ($p=0.01$) elicited a significant dose-dependent oxidative response in lung macrophages which was lower in WNiFe-exposed cells compared to WNiCo-exposed cells at all concentrations tested ($p<0.05$; Fig. 7). The ROS/RNS formation induced by WNiCo was significantly greater than that induced by the individual metal components, especially at the higher concentrations shown to be toxic to lung macrophages *in vitro* (100 and 200 μg/ml), suggesting a synergistic effect. When pure metals were investigated, only W and Co produced detectable levels of ROS/RNS, with Co eliciting a greater response (Fig. 7).

Effect of WNiCo exposure on phagocytosis

Phagocytosis of nonopsonized zymosan particles was reduced in lung macrophages exposed to ≥25 μg/ml WNiCo ($p=0.02$), and ≥50 μg/ml WNiFe ($p=0.004$; Fig. 8). Maximal reduction in absorbance was 17% that of untreated cells for WNiCo and 19% for WNiFe. Phagocytosis of WNiCo and WNiFe particles and zymosan by lung macrophages was visually confirmed in a subset of cells using microscopy (not shown).

Discussion

Very few studies exist which investigate the cellular and molecular mechanisms associated with the effects of inhalation exposure to HMTAs despite the recognized risk of this route of exposure to military personnel (Gold et al., 2007; Machado et al., 2010, 2011). Results from this study determined that *in vivo* exposure to military-relevant reconstituted HMTA mixtures consisting of 92% W/5% Ni/3% Co and 92% W/5% Ni/3% Fe induces pulmonary inflammation and altered expression of genes associated with oxidative and metabolic stress and toxicity in the rat. Inhalation exposure to both WNiCo and WNiFe likely causes lung injury by inducing macrophage activation, neutrophilia, and the generation of toxic oxygen radicals. The higher degree of oxidative stress induced by WNiCo compared to WNiFe may contribute to its increased toxicity and carcinogenicity observed *in vivo* (Harris et al., 2011; Kalinich et al., 2005; Roszell et al., 2008).

Pure tungsten and its compounds traditionally have not been considered very toxic to humans and have been used as a component in US Food and Drug Administration-approved medical implants without adverse effects (van der Voet et al., 2007). Although exposure to hard metal dust, which is composed of tungsten carbide and Co, has been associated with fibrosing alveolitis (hard metal lung disease) and lung cancer (De Boeck et al., 2003; Huaux et al., 1995; Lison and Lauwerys, 1994; Stefaniak et al., 2009; Wild et al., 2009), the majority of its toxicity is thought to be attributable to the effects of Co (van der Voet et al., 2007). Generation of ROS by Co and/or tungsten carbide is implicated in causing hard metal lung disease and allergic contact dermatitis (Lison et al., 1995; Stefaniak et al., 2010). Ni and Co by themselves are known to be associated with cancer development, and mixtures of Ni and Co chlorides induce a synergistic toxic response in alveolar epithelial type II cells (Cross et al., 2001; Lison et al., 2001; Lu et al., 2005). While the primary route of toxicity for Ni is the depletion of glutathione and bonding to sulfhydryl groups of proteins which may inhibit active centers of key enzymes, it is well established that Co-mediated free radical generation contributes to the toxicity and carcinogenicity of Co (Valko et al., 2005).

The formation of ROS and RNS is a common factor in determining the toxicity and carcinogenicity of metals, and oxidative stress is known to contribute to the pathophysiology of heavy metal exposure (Valko et al., 2005). Oxidative stress is a condition whereby the production of oxygen radicals exceeds the threshold for antioxidant neutralization by non-enzymatic antioxidants such as glutathione or by antioxidant enzymes including glutathione peroxidase and superoxide dismutase (Flora, 2009). Evidence of HMTA-induced oxidative stress in the rat lung after *in vivo* exposure was demonstrated by a marked induction of nitric oxide synthase type 2 (Nos2/iNOS) mRNA, which encodes an inducible enzyme that produces nitric oxide. Compared to saline-exposed animals, WNiCo induced a remarkable 49-fold increase in Nos2/iNOS mRNA expression in BAL cells, while WNiFe induced a 14-fold increase. The Nos2/iNOS mRNA levels corresponded with intracellular ROS/RNS formation elicited by WNiCo and WNiFe; the oxidative burst response was significantly lower in WNiFe-exposed cells than WNiCo-exposed cells at all concentrations evaluated.

At doses which reduced metabolic viability of BAL cells *in vitro* (100 and 200 μg/ml), WNiCo (and to a much lesser extent, WNiFe) induced a rapid dose-dependent oxidative burst that was greater than the combined responses of the individual metals, suggesting that an interaction between the constituents of the alloy enhanced the intracellular production of ROS/RNS. The oxidative burst response was greatest for Co, was detectable at low levels for W, and was virtually

undetectable for Ni and Fe when individual metals comprising the tungsten alloys were compared. These data support the findings of Harris et al. (2011), who suggested that this synergistic effect is likely increased by the biphasic nature of the alloy in which the presence of pure tungsten particles will cause a preferential corrosion of the binder matrix.

HMTA particle-derived ROS (Harris et al., 2011) may react with cell-derived ROS and RNS (produced by phagocytic BAL cells attempting to digest the HMTA particles) yielding additional toxic species including peroxynitrite from nitric oxide and superoxide anion (Fubini and Hubbard, 2003). Detrimental cellular effects of ROS and RNS in the lung may include damage to cell membranes by lipid peroxidation, damage to target cell DNA, oxidation of proteins, and altered calcium and sulfhydryl homeostasis (Schins and Borm, 1999; Valko et al., 2005). Furthermore, ROS can cause additional acute injury to the lungs by inducing the production of inflammatory mediators through activation of the nuclear factor kappa B signaling pathway (Storz et al., 2004). Genotoxicity may be caused by the direct actions of the WNiCo and WNiFe particles (Miller et al., 2001) or indirect mechanisms mediated by ROS and RNS produced by inflammatory cells (Martin et al., 1997). In fact, excessive and persistent formation of ROS is believed to cause the indirect genotoxicity of particles following exposure to high concentrations of poorly soluble dust (Schins, 2002). In a prior study, exposure to DU particles inhaled by rats was shown to result in DNA strand breaks in BAL cells and an increase in inflammatory cytokine expression and the production of hydroperoxides in lung tissue, suggesting that DU-induced DNA damage was a consequence of the inflammatory processes and oxidative stress (Monleau et al., 2006).

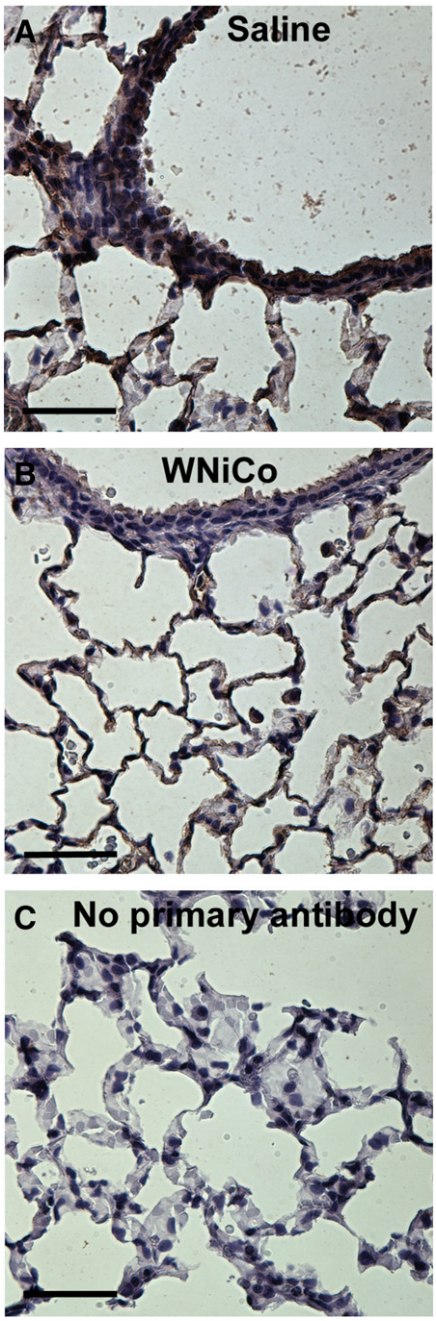

Fig. 6. CYP2A3 expression in rat lung tissue 24 h after intratracheal instillation of (A) saline or (B) WNiCo (2 mg/100 g body weight). C. No CYP2A antibody (negative control). Note reduced expression in bronchiolar epithelium in WNiCo-exposed lung. Original magnification ×640, bar = 50 μm.

Inhaled particulates reach predominantly two types of cells, lung macrophages and epithelial cells (Schins and Borm, 1999). Alveolar macrophages constitute an important and primary line of defense against inhaled pathogens and play a key role in clearing particulate matter from the lungs by phagocytosis (Brain, 1992). The engulfment of micrometer-sized particles by macrophages in the lung is rapid and the process is usually completed within 24 h (Alexis et al., 2006). Classically activated macrophages produce proinflammatory cytokines such as TNF-α and IL-6, proteolytic enzymes, growth factors, and a marked upregulation of Nos2/iNOS associated with toxic nitric oxide production that together help to destroy phagocytosed pathogens (Mosser and Edwards, 2008). Although they are known to perform many other protective functions and act as modulators of the immune response, these macrophages may also contribute to tissue injury when activated and/or damaged (Brain, 1992). Target cells such as bronchiolar and alveolar epithelial cells may be affected by both the macrophage products and the extracellular particles, resulting in activation and/or cell death (Brain, 1992; Fubini and Hubbard, 2003).

Findings from this study determined that alveolar macrophage interaction with WNiCo and WNiFe particles results in particle phagocytosis, macrophage activation, and ROS/RNS production. The release of inflammatory mediators by these macrophages causes the recruitment and activation of additional macrophages, neutrophils, and lymphocytes, which may subsequently lead to tissue injury. Evidence of lung injury is well documented in patients with hard metal lung disease caused by exposure to dust composed of tungsten carbide and Co (Moriyama et al., 2007). It is thought that macrophages may phagocytose inhaled tungsten via CD163, and together with cytotoxic T lymphocytes, are primarily responsible for the formation of fibrotic lesions manifested in hard metal lung disease (Moriyama et al., 2007).

Table 2
Effect of metal treatment on viability of rat lung macrophages *in vitro* (5×10^4 cells/well). Data were normalized to values obtained for untreated cells and are presented as % control (SEM). The concentrations of individual metals were the equivalent amounts present in the tungsten alloys. Assays were performed in triplicate wells and include determinations from three separate experiments.

Concentration (μg/ml)	WNiCo	WNiFe	W	Ni	Co	Fe
12.5	87(5)	104(10)	79(4)	82(3)	92(5)	88(5)
25	91(2)	102(13)	90(11)	86(1)[a]	89(4)	107(13)
50	95(3)	93(10)	86(15)	93(2)	95(4)	107(1)
100	66(8)[a]	60(4)[a]	54(6)[a]	91(6)	90(3)	98(7)
200	42(17)[a]	27(13)[a]	49(3)[a]	88(4)[a]	84(3)	100(6)
400	38(8)[a]	36(22)[a]	18(10)[a]	94(1)	92(1)	108(4)
1000	11(5)[a]	17(3)[a]	9(6)[a]	86(3)[a]	81(7)	94(5)
p value[b]	<0.001	<0.001	<0.001	0.02	0.07	0.09

[a] $p<0.05$, ANOVA followed by multiple comparisons versus the untreated group (Holm–Sidak method).
[b] ANOVA, overall concentration-associated effect.

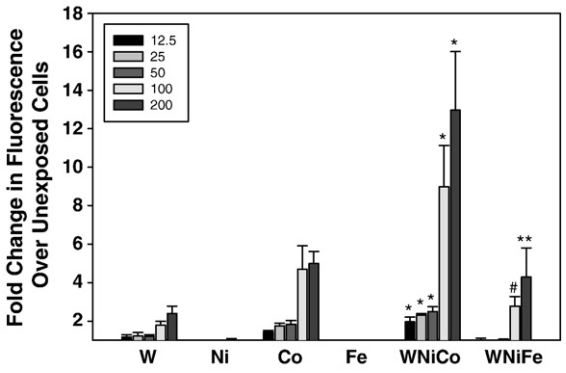

Fig. 7. Intracellular ROS/RNS generation in rat lung macrophages 1 h after exposure to 12.5–200 μg/ml WNiCo, WNiFe, or equivalent amount of W, Ni, Co, and Fe used in the tungsten alloys. Values represent the mean ± SEM of 4 separate experiments assayed in triplicate wells. *$p<0.05$ compared to W, Ni, and Co at their respective concentrations; ANOVA followed by multiple comparisons vs. WNiCo (Holm–Sidak method). **$p<0.05$ compared to W, Ni, and Fe at their respective concentrations; #$p<0.05$ compared to Ni and Fe at their respective concentrations; ANOVA followed by multiple comparisons vs. WNiFe (Holm–Sidak method).

Whether inhalation exposure to HMTAs causes a functional impairment of the anti-pathogenic capability of lung macrophages is currently unknown. Preliminary results in this study determined that *in vitro* WNiCo and WNiFe exposure caused a statistically significant decrease in the phagocytosis of zymosan particles by BAL macrophages at concentrations which included those that did not reduce metabolic viability. This finding may have important implications for soldiers deployed in the Middle East, given the detection of potentially viable pathogens in breathable dust samples from Kuwait and Iraq (Leski et al., 2011). Pulmonary exposure to airborne particulates has been shown to alter lung macrophage function and may lead to increased susceptibility to lung infection (Antonini et al., 2002; Schwartz, 1996; Zhou and Kobzik, 2007). Additional research is needed to determine whether the pulmonary host defense is altered in military personnel after acute exposure to aerosolized HMTA particles, and which metal combinations in the alloys, if any, may be responsible for an increased susceptibility to infection.

Altered expression in BAL cells of several genes that play a key role in regulating inflammation, cell cycle progression, cell proliferation, apoptosis signaling, heat shock, and/or DNA damage and repair was found to occur in response to WNiCo and WNiFe (listed in Table 1). The mRNA expression levels for many of these genes greatly exceeded those from animals instilled with the individual metals, suggesting a synergistic effect. Genes primarily involved in inflammation and growth arrest and senescence were identified as being differentially expressed in both alloys. One such gene whose expression was increased nearly 6-fold in WNiCo-exposed BAL cells and 8-fold in WNiFe-exposed cells is Cdkn1a (cyclin-dependent kinase inhibitor 1A), which encodes $p21^{CIP1/WAF1}$, an important inhibitory regulator of cell cycle progression highly responsive to oxidative stress (Tomita et al., 2002). This protein is increased in alveolar macrophages and biopsies from smokers and is associated with reduced apoptosis (Tomita et al., 2002). Likewise, Chek2 (checkpoint kinase 2), which encodes a multifunctional kinase enzyme involved in the induction of cell cycle arrest, DNA repair, and apoptosis, and whose defects have been associated with increased breast cancer risk (Tung and Silver, 2011), was downregulated greater than 3.5-fold in WNiFe-exposed BAL cells and nearly 2-fold in WNiCo-exposed cells. Reduced apoptosis can result in prolonged cellular activation of lung macrophages, may impair the removal of abnormal cells resulting from improper DNA repair, and has implications in the carcinogenic potential of WNiCo and WNiFe (Harris et al., 2011; Miller et al., 2001).

Interestingly, WNiFe induced a greater heat shock response than WNiCo, whereby the expression of four genes encoding heat shock proteins was upregulated after exposure to WNiFe compared to one gene in response to WNiCo. In the lungs, heat shock protein expression is induced by various stimuli, including oxidative stress, and is an endogenous, protective mechanism against acute lung inflammation (Kopczynska et al., 2011; Malago et al., 2002; Shi et al., 2006). Heat shock proteins act as molecular chaperones that protect cells from the cytotoxic effects of protein misfolding and aggregation, and they also downregulate proinflammatory cytokine production by interfering with the nuclear factor kappa B and mitogen-activated protein kinase pathways (Malago et al., 2002). The elevated heat shock response induced by WNiFe compared to WNiCo may contribute to the reduced toxicity of WNiFe observed not only in this study (indicated by the reduced albumin content and trend toward decreased LDH activity in the BAL fluid from WNiFe-exposed animals), but also by others (Harris et al., 2011; Roszell et al., 2008).

Despite the altered expression of several stress and toxicity genes induced in BAL cells after the intratracheal instillation of WNiCo, only 2 genes were identified as being differentially expressed in whole lung tissue. These included IL-6 and CYP2A3, a cytochrome P450 enzyme preferentially expressed in the respiratory tract. Homogenized intact lungs contain a mixture of epithelial, endothelial, and inflammatory cells (predominantly neutrophils and macrophages) among other cell types, and therefore mRNA analyses using a whole lung preparation may mask cell-specific molecular responses. Nevertheless, WNiCo was found to induce a remarkable 42-fold decrease in the mRNA expression of CYP2A3, which is the rat ortholog of human CYP2A13 known to be highly active in the metabolic activation of tobacco-specific nitrosamines and implicated in smoking-induced lung cancer (Ling et al., 2004). Downregulation of CYP2A3 protein was also evident in immunohistochemically-stained sections of lung tissue from WNiCo-

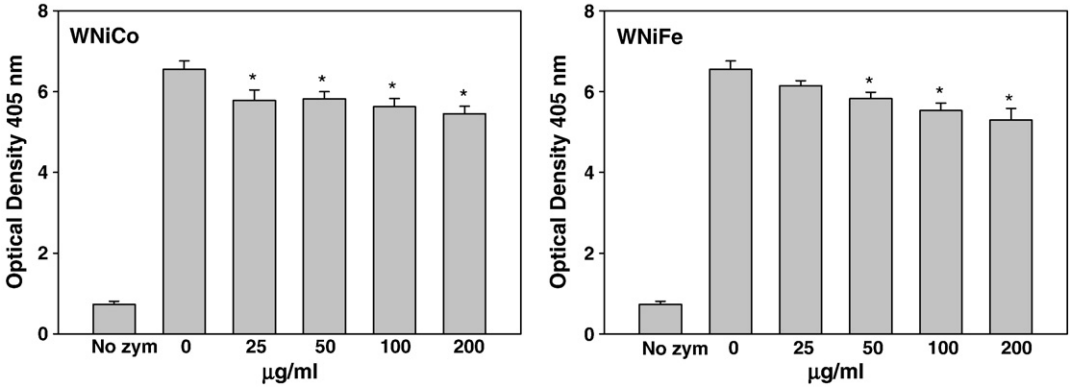

Fig. 8. Phagocytosis of zymosan particles by rat lung macrophages after exposure to 25–200 μg/ml WNiCo or WNiFe. Values represent the mean ± SEM of 4 separate experiments assayed in triplicate wells. *$p<0.05$ compared to untreated cells; ANOVA followed by multiple comparisons vs. the control (0 μg/ml) group.

instilled rats, particularly in the bronchiolar epithelium. Ni appeared to contribute the greatest effect relative to the other alloy components, because the instillation of Ni at a concentration present in the tungsten alloy resulted in a 36-fold decrease in CYP2A3 expression. In contrast, CYP2A3 mRNA expression was not found to be significantly altered in BAL cells after the intratracheal instillation of WNiCo, WNiFe, or individual metals at concentrations present in the tungsten alloys.

Cytochrome P450 suppression is a pathophysiological response to stress signals such as those elicited by inflammation, infection, or toxins (Riddick et al., 2004). Transcriptional repression is a primary mechanism for downregulation of hepatic P450 mRNAs in the acute phase of infection and inflammation, although relatively little data exist on the effects of inflammation or infection on extrahepatic P450 expression (Morgan, 2001; Riddick et al., 2004). Inflammation induced by respirable coal dust particles was associated with downregulation of CYP1A1 in the lung (Ghanem et al., 2004), and oxidative stress has been shown to downregulate the CYP1A1 gene promoter through the transcription factor nuclear factor 1 (Morel and Barouki, 1998). Proposed mechanisms responsible for the observed decrease in CYP2A3 mRNA and protein expression include i) the release of proinflammatory cytokines from activated macrophages and other lung cells results in the modulation of transcription factors, leading to a downregulation of CYP2A3 (Ling et al., 2004, 2007; Morgan, 2001); ii) the production of cytokines also activates Nos2/iNOS to form nitric oxide that inhibits P450 enzyme activities directly and/or leads to the downregulation of CYP2A3 protein via destabilization (Morgan, 2001); and iii) Ni or Co ions themselves are capable of affecting CYP2A3 expression by a transcriptional, post-transcriptional, or post-translational mechanism.

In conclusion, findings from this study determined that the intratracheal instillation of WNiCo and WNiFe causes lung injury by inducing pulmonary inflammation and the generation of toxic oxygen radicals. We propose that the rapid intracellular ROS/RNS formation induced by WNiCo, and to a lesser extent, WNiFe, may also lead to a gradual depletion of energy stores and subsequent diminished oxidative burst response and phagocytosis capability of lung macrophages, thereby compromising their defensive role. Because this may have important implications for military personnel deployed in the Middle East, given the detection of potentially viable pathogens in breathable dust samples from Kuwait and Iraq (Leski et al., 2011), additional research investigating the effects of HMTAs on pulmonary host defense is vastly needed. Results from this study emphasize the need for postdeployment medical surveillance programs relevant to aerosolized metals that monitor pulmonary function and accumulated burden of metals in various tissues. The investigation of additional metal combinations used in HMTA development is warranted.

Conflict of interest statement

The authors declare that there are no conflicts of interest.

Acknowledgments

This work was funded by a Defense Medical Research and Development Program grant awarded to LP. The sponsor had no involvement in study design; in the collection, analysis, and interpretation of data; in the writing of the manuscript; or in the decision to submit the paper for publication. We thank Lee-Ann Murata and Claudia Hernandez for technical assistance with some of the BAL fluid assays.

References

Alexis, N.E., Lay, J.C., Zeman, K.L., Geiser, M., Kapp, N., Bennett, W.D., 2006. *In vivo* particle uptake by airway macrophages in healthy volunteers. Am. J. Respir. Cell Mol. Biol. 34, 305–313.

Antonini, J.M., Roberts, J.R., Jernigan, M.R., Yang, H.M., Ma, J.Y.C., Clarke, R.W., 2002. Residual oil fly ash increases the susceptibility to infection and severely damages the lungs after pulmonary challenge with a bacterial pathogen. Toxicol. Sci. 70, 110–119.

Brain, J.D., 1992. Mechanisms, measurement, and significance of lung macrophage function. Environ. Health Perspect. 97, 5–10.

Brain, J.D., Knudson, D.E., Sorokin, S.P., Davis, M.A., 1976. Pulmonary distribution of particles given by intratracheal instillation or by aerosol inhalation. Environ. Res. 11, 13–33.

Cross, D.P., Ramachandran, G., Wattenberg, E.V., 2001. Mixtures of nickel and cobalt chlorides induce synergistic cytotoxic effects: implications for inhalation exposure modeling. Ann. Occup. Hyg. 45, 409–418.

De Boeck, M., Hoet, P., Lombaert, N., Nemery, B., Kirsch-Volders, M., Lison, D., 2003. *In vivo* genotoxicity of hard metal dust: induction of micronuclei in rat type II epithelial lung cells. Carcinogenesis 24, 1793–1800.

Flora, S.J.S., 2009. Structural, chemical and biological aspects of antioxidants for strategies against metal and metalloid exposure. Oxid. Med. Cell. Longev. 2, 191–206.

Fubini, B., Hubbard, A., 2003. Reactive oxygen species (ROS) and reactive nitrogen species (RNS) generation by silica in inflammation and fibrosis. Free Radical Biol. Med. 34, 1507–1516.

Ghanem, M.M., Porter, D., Battelli, L.A., Vallyathan, V., Kashon, M.L., Ma, J.Y., Barger, M.W., Nath, J., Castranova, V., Hubbs, A.F., 2004. Respirable coal dust particles modify cytochrome P4501A1 (CYP1A1) expression in rat alveolar cells. Am. J. Respir. Cell Mol. Biol. 31, 171–183.

Gold, K., Cheng, Y.S., Holmes, T.D., 2007. A quantitative analysis of aerosols inside an armored vehicle perforated by a kinetic energy penetrator containing tungsten, nickel, and cobalt. Mil. Med. 172, 393–398.

Harris, R.M., Williams, T.D., Hodges, N.J., Waring, R.H., 2011. Reactive oxygen species and oxidative DNA damage mediate the cytotoxicity of tungsten–nickel–cobalt alloys *in vitro*. Toxicol. Appl. Pharmacol. 250, 19–28.

Huaux, F., Lasfargues, G., Lauwerys, R., Lison, D., 1995. Lung toxicity of hard metal particles and production of interleukin-1, tumor necrosis factor-alpha, fibronectin, and cystatin-c by lung phagocytes. Toxicol. Appl. Pharmacol. 132, 53–62.

Kalinich, J.F., Emond, C.A., Dalton, T.K., Mog, S.R., Coleman, G.D., Kordell, J.E., Miller, A.C., McClain, D.E., 2005. Embedded weapons-grade tungsten alloy shrapnel rapidly induces metastatic high-grade rhabdomyosarcomas in F344 rats. Environ. Health Perspect. 113, 729–734.

Kalinich, J.F., Vergara, V.B., Emond, C.A., 2008. Urinary and serum metal levels as indicators of embedded tungsten alloy fragments. Mil. Med. 173, 754–758.

Kane, M.A., Kasper, C.E., Kalinich, J.F., 2009. Protocol for the assessment of potential health effects from embedded metal fragments. Mil. Med. 174, 265–269.

Kopczynska, B., Sulejczak, D., Welniak-Kaminska, M., Gietka, A., Grieb, P., 2011. Anandamide enhances expression of heat shock proteins Hsp70 and Hsp25 in rat lungs. Eur. J. Pharmacol. 668, 257–263.

Leski, T.A., Malanoski, A.P., Gregory, M.J., Lin, B., Stenger, D.A., 2011. Application of broad-range resequencing array RPM-TEI for detection of pathogens in desert dust samples from Kuwait and Iraq. Appl. Environ. Microbiol. 77, 4285–4292.

Ling, G., Hauer, C.R., Gronostajski, R.M., Pentecost, B.T., Ding, X., 2004. Transcriptional regulation of rat *CYP2A3* by nuclear factor 1. J. Biol. Chem. 279, 27888–27895.

Ling, G., Wei, Y., Ding, X., 2007. Transcriptional regulation of human *CYP2A13* expression in the respiratory tract by CCAAT/enhancer binding protein and epigenetic modulation. Mol. Pharmacol. 71, 807–816.

Lison, D., Lauwerys, R., 1994. Cobalt bioavailability from hard metal particles. Further evidence that cobalt alone is not responsible for the toxicity of hard metal particles. Arch. Toxicol. 68, 528–531.

Lison, D., Carbonnelle, P., Mollo, L., Lauwerys, R., Fubini, B., 1995. Physiochemical mechanism of the interaction between cobalt metal and carbide particles to generate toxic activated oxygen species. Chem. Res. Toxicol. 8, 600–606.

Lison, D., De Boeck, M., Veroughstraete, V., Kirsch-Volders, M., 2001. Update on the genotoxicity and carcinogenicity of cobalt compounds. Occup. Environ. Med. 58, 619–625.

Lu, H., Shi, X., Costa, M., Huang, C., 2005. Carcinogenic effect of nickel compounds. Mol. Cell. Biochem. 279, 45–67.

Machado, B.I., Murr, L.E., Suro, R.M., Gaytan, S.M., Ramirez, D.A., Garza, K.M., Schuster, B.E., 2010. Characterization and cytotoxic assessment of ballistic aerosol particulates for tungsten alloy penetrators into steel target plates. Int. J. Environ. Res. Public Health 7, 3313–3331.

Machado, B.I., Suro, R.M., Garza, K.M., Murr, L.E., 2011. Comparative microstructures and cytotoxicity assays for ballistic aerosols composed of micrometals and nanometals: respiratory health implications. Int. J. Nanomed. 6, 167–178.

Malago, J.J., Koninkx, J.F.J.G., van Dijk, J.E., 2002. The heat shock response and cytoprotection of the intestinal epithelium. Cell Stress Chaperones 7, 191–199.

Martin, L.D., Krunkosky, T.M., Dye, J.A., Fischer, B.M., Jiang, N.F., Rochelle, L.G., Akley, N.J., Dreher, K.L., Adler, K.B., 1997. The role of reactive oxygen and nitrogen species in the response of airway epithelium to particulates. Environ. Health Perspect. 105 (Suppl. 5), 1301–1307.

Miller, A.C., McClain, D., 2007. A review of depleted uranium biological effects: *in vitro* and *in vivo* studies. Rev. Environ. Health 22, 75–89.

Miller, A.C., Mog, S., McKinney, L., Luo, L., Allen, J., Xu, J., Page, N., 2001. Neoplastic transformation of human osteoblast cells to the tumorigenic phenotype by heavy metal-tungsten alloy particles: induction of genotoxic effects. Carcinogenesis 22, 115–125.

Miller, A.C., Xu, J., Stewart, M., Prasanna, P.G., Page, N., 2002. Potential late health effects of depleted uranium and tungsten used in armor-piercing munitions: comparison of neoplastic transformation and genotoxicity with the known carcinogen nickel. Mil. Med. 167 (2 Suppl.), 120–122.

Miller, A.C., Brooks, K., Smith, J., Page, N., 2004. Effect of the militarily-relevant heavy metals, depleted uranium and heavy metal tungsten-alloy on gene expression in human liver carcinoma cells (HepG2). Mol. Cell. Biochem. 255, 247–256.

Monleau, M., De Meo, M., Paquet, F., Chazel, V., Dumenil, G., Donnadieu-Claraz, M., 2006. Genotoxic and inflammatory effects of depleted uranium particles inhaled by rats. Toxicol. Sci. 89, 287–295.

Morel, Y., Barouki, R., 1998. Down-regulation of cytochrome P450 1A1 gene promoter by oxidative stress. Critical contribution of nuclear factor 1. J. Biol. Chem. 273, 26969–26976.
Morgan, E.T., 2001. Regulation of cytochrome P450 by inflammatory mediators: why and how? Drug Metab. Dispos. 29, 207–212.
Moriyama, H., Kobayashi, M., Takada, T., Shimizu, T., Terada, M., Narita, J., Maruyama, M., Watanabe, K., Suzuki, E., Gejyo, F., 2007. Two dimensional analysis of elements and mononuclear cells in hard metal lung disease. Am. J. Respir. Crit. Care Med. 176, 70–77.
Mosser, D.M., Edwards, J.P., 2008. Exploring the full spectrum of macrophage activation. Nat. Rev. Immunol. 8, 958–969.
Mukaida, N., 2003. Pathophysiological roles of interleukin-8/CXCL8 in pulmonary diseases. Am. J. Physiol. Lung Cell. Mol. Physiol. 284, L566–L577.
Ogundipe, A., Greenberg, B., Braida, W., Christodoulatos, C., Dermatas, D., 2006. Morphological characterization and spectroscopic studies of the corrosion behavior of tungsten heavy alloys. Corros. Sci. 48, 3281–3297.
Parkhurst, M.A., Guilmette, R.A., 2009. Conclusions of the Capstone depleted uranium aerosol characterization and risk assessment study. Health Phys. 96, 393–409.
Pierce, L.M., Alessandrini, F., Godleski, J.J., Paulauskis, J.D., 1996. Vanadium-induced chemokine mRNA expression and pulmonary inflammation. Toxicol. Appl. Pharmacol. 138, 1–11.
Riddick, D.S., Lee, C., Bhathena, A., Timsit, Y.E., Cheng, P.Y., Morgan, E.T., Prough, R.A., Ripp, S.L., Miller, K.K., Jahan, A., Chiang, J.Y.L., 2004. Transcriptional suppression of cytochrome P450 genes by endogenous and exogenous chemicals. Drug Metab. Dispos. 32, 367–375.
Roszell, L.E., Hess-Ruth, A., Beall, P., Catherine, P., 2008. Health effects of embedded fragments of tungsten and tungsten alloys. Toxicologist 102, 2101.
Schins, R.P., 2002. Mechanisms of genotoxicity of particles and fibers. Inhal. Toxicol. 14, 57–78.
Schins, R.P., Borm, P.J., 1999. Mechanisms and mediators in coal dust induced toxicity: a review. Ann. Occup. Hyg. 43, 7–33.
Schwartz, J., 1996. Air pollution and hospital admissions for respiratory disease. Epidemiology 7, 20–28.
Shi, Y., Tu, Z., Tang, D., Zhang, H., Liu, M., Wang, K., Calderwood, S.K., Xiao, X., 2006. The inhibition of LPS-induced production of inflammatory cytokines by HSP70 involves inactivation of the NF-kappaB pathway but not the MAPK pathways. Shock 26, 277–284.
Stefaniak, A.B., Virji, M.A., Day, G.A., 2009. Characterization of exposures among cemented tungsten carbide workers. Part I. Size-fractionated exposures to airborne cobalt and tungsten particles. J. Exposure Sci. Environ. Epidemiol. 19, 475–491.
Stefaniak, A.B., Harvey, C.J., Bukowski, V.C., Leonard, S.S., 2010. Comparison of free radical generation by pre- and post-sintered cemented carbide particles. J. Occup. Environ. Hyg. 7, 23–34.
Storz, P., Doppler, H., Toker, A., 2004. Protein kinase Cdelta selectively regulates protein kinase D-dependent activation of NF-kappaB in oxidative stress signaling. Mol. Cell. Biol. 24, 2614–2626.
Thompson, A.B., Teschler, H., Wang, Y.M., Konietzko, N., Costabel, U., 1996. Preparation of bronchoalveolar lavage fluid with microscope slide smears. Eur. Respir. J. 9, 603–608.
Tomita, K., Caramori, G., Lim, S., Ito, K., Hanazawa, T., Oates, T., Chiselita, I., Jazrawi, E., Chung, K.F., Barnes, P.J., Adcock, I.M., 2002. Increased $p21^{CIP1/WAF1}$ and B cell lymphoma leukemia-x_L expression and reduced apoptosis in alveolar macrophages from smokers. Am. J. Respir. Crit. Care Med. 166, 724–731.
Tung, N., Silver, D.P., 2011. Chek2 DNA damage response pathway and inherited breast cancer risk. J. Clin. Oncol. doi:10.1200/JCO.2011.37.1476
Valko, M., Morris, H., Cronin, M.T.D., 2005. Metals, toxicity, and oxidative stress. Curr. Med. Chem. 12, 1161–1208.
van der Voet, G.B., Todorov, T.I., Centeno, J.A., Jonas, W., Ives, J., Mullick, F.G., 2007. Metals and health: a clinical toxicological perspective on tungsten and review of the literature. Mil. Med. 172, 1002–1005.
Wild, P., Bourgkard, E., Paris, C., 2009. Lung cancer and exposure to metals: the epidemiological evidence. Methods Mol. Biol. 472, 139–167.
Zhou, H., Kobzik, L., 2007. Effect of concentrated ambient particles on macrophage phagocytosis and killing of *Streptococcus pnuemoniae*. Am. J. Respir. Cell Mol. Biol. 36, 460–465.